PCCP

Ion and Water Transport Reasonably Involves Rotation and Pseudorotation: Measurement and Modeling the Temperature Dependence of Small-Angle Neutron Scattering from Aqueous SrI_2

Journal:	*Physical Chemistry Chemical Physics*
Manuscript ID	CP-ART-04-2020-002088.R1
Article Type:	Paper
Date Submitted by the Author:	26-May-2020
Complete List of Authors:	Rubinson, Kenneth; NIST, NCNR; Wright State University, Department of Biochemistry and Molecular Biology, Mountain, Raymond D.; NIST, Physics

Ion and Water Transport Reasonably Involves Rotation and Pseudorotation: Measurement and Modeling the Temperature Dependence of Small-Angle Neutron Scattering from Aqueous SrI_2

Kenneth A. Rubinson* [a,b], Raymond D. Mountain[c]

a. Department of Biochemistry and Molecular Biology, Wright State University, Dayton, OH 45435
b. NIST Center for Neutron Research, National Institute of Standards and Technology, Gaithersburg, MD 20899
c. Chemical Sciences Division, National Institute of Standards and Technology, Gaithersburg, MD 20899

Author□s email: Rubinson@wright.edu, Rubinson@nist.gov, raymond.mountain@nist.gov

Key words: Ionic solution structure, solution prepeak, SANS, correlation length, ion transport, proton exchange rate, pseudorotation

Abstract

X-ray and neutron scattering have provided insight into the short range (<8 Å) structures of ionic solutions for over a century. For longer distances, single scattering bands have, however, been seen. For the non-hydrolyzing salt SrI_2 in aqueous (D_2O) solution, a structure sufficient to scatter slow neutrons has been seen to persist down to a concentration of 0.1 mol L^{-1} where the measured average spacing between scatterers is over 20 Å. Theoretical studies of such long distance solution structures are difficult, and these difficulties are discussed. The width of the distribution in distances between the scatterers (ions, ion pairs, etc.) remains less than 10 Å, which approximates the average size of the ions and their first hydration shell. Here, we measure the temperature dependence from 10EC to 90EC of the small angle neutron scattering (SANS) by a 0.5 molar SrI_2 solution in D_2O and find that this surprisingly narrow distribution of the distances remains constant within experimental uncertainty. This structure of the ions in the solution appears to endure because changes in interion distances along any single spatial dimension require displacements near the size of a water molecule. Together, the experimental measurements support a rotatory mechanism for simultaneous ion transport and water countertransport. Since rotation minimizes displacement of the solution framework, it is suggested that water transport alone also involves rotation of multimolecular structures, and that the interpretation of single-molecule water rotation is confounded by pseudorotation that results from paired picosecond proton exchanges. It is pointed out that NMR-determined millisecond to microsecond proton exchange times of chelated-metal-ion bound waters and the much faster chelate rotational correlation times around 10 picoseconds, both of which require making and breaking of hydrogen bonds, are difficult to impossible to reconcile.

I. **Introduction**

Small angle scattering of cold neutrons (SANS) from solutions gives experimental access to structures with lengths on the order of 10 Å and longer where there is contrast present between the solvent and the solute. (The contrast may be considered as differences in the neutrons index of refraction for the solvent and solute.) Since solution structures over these length scales only can be probed directly by small angle scattering, such experiments offer the possibility of new insights for molecular behavior.[1] A great benefit of SANS is that the information provided is for the average structures between ionic species since any water structural correlations occur at distances shorter than the cutoff of the measurements.

The SANS data can be described as the sum of the scattering between pairs of scatterers with correlated spatial positions at each of the lengths in the range probed by the experiments.[2] This is labeled coherent scattering. One benefit from the idea of spatial correlation is that it can express structures on a continuum from stiff, highly structured entities (correlation unity) through unstructured (correlation zero).

For ionic solutions, the coherent scattering results from rotationally randomly oriented structures in the solvent. In other words, the solution consists of a set of distinct scattering units that has a correlated structure embedded in an uncorrelated solvent environment. For the aqueous (here, D_2O) solution of 0.5 M SrI_2 (M = mol L^{-1}), which is the subject of this work, the scattering shows a single peak in the plot of the scattering intensity $I(q)$ versus q (where $q = (4\pi/\lambda)\cong\sin\theta$, and 2θ is the scattering angle measured from the axis of the incoming neutron flux). For this study, SrI_2 in D_2O was chosen because both the Sr^{2+} and I^- scatter neutrons, and hydrolysis can be neglected; the solutions have near neutral pDs at all concentrations.

The experimental peaks are well fit by Lorentzian curves where the peak can be related to the distance d between scatterers by $d = 2\pi/q_{peak}$. In addition the halfwidth at half height of the Lorentzian provides the spatial correlation length between the scatterers, which is on the order of an Å.

The question addressed here is how to resolve the conflict between having a structure so rigid that it can scatter neutrons and yet can allow the transport processes of diffusion and ionic conduction. As will be discussed, the structure and motion results appear to be consistent only when the ion transport is a consequence of rotations of ion-water constructs consisting of ions with partial hydration layers together having an approximately circular cross section to bring about the ion transport and solvent countertransport.

II. Materials and Methods*

II.1 *Strontium iodide solutions*: At least 24 hours before the scattering experiment, anhydrous SrI_2 (99.99% metals based, Alfa Aesar, Ward Hill, MA) was both measured out and weighed in a dry N_2 atmosphere. D_2O (99.9%, Cambridge Isotope Labs) was added to produce a 2.00 M solution. The appropriate D_2O volume was calculated by subtracting the volume of the salt from the desired total volume, since the densities of aqueous SrI_2 solutions were found to be reproduced by the reverse of this calculation using the density of solid, anhydrous SrI_2, which is 4.55 g cm^{-3}. The experimental 0.500 M solution was prepared by diluting the stock. A small amount of solids was removed by passing the solution through a 0.2 μm filter. Before running, the solution was degassed by heating to 70 EC for an hour and removing the bubbles that appeared.

As noted above, both the anion and cation species scatter, and their scattering length densities are approximately equal. Using the density of Sr metal (2.65 g cm^{-3}) and the density of I_2 liquid (4.933 g cm^{-3}), the NIST Center for Neutron Research (NCNR) scattering length density (SLD) calculator (http://www.ncnr.nist.gov/resources/sldcalc.html) gives the strontium SLD as 1.28 H 10^{-6} A^{-2} and that for iodide as 1.24 H 10^{-6} A^{-2}. Some adjustment for the differences between the atomic and ionic dimensions and the solvent electrostriction would be necessary to find more accurate values. Nevertheless, the cations and anions scatter nearly equally.

The pD value was recorded by a glass electrode calibrated in H_2O. No isotope correction was made with the assumption that the unmodified value was more accurate since it is likely that the buffer pD and electrode surface□s pK_a shifted approximately the same amount with the level of D-H substitution.[3] Solutions 0.5 M in SrI_2 in D_2O have pD values 7.4 ∀ 0.1 at ambient temperature.

II.2. *Small-angle neutron scattering (SANS) data collection:* The SrI_2 solutions were held in (2.00 ∀ 0.1) mm pathlength cylindrical silica spectrometry cells (Hellma, Plainview, NY) with a volume ~640 μL. SANS measurements were performed on the NG7 30 m SANS instruments at the NCNR in Gaithersburg, MD.[4] Data was collected for both the SrI_2 solution and the D_2O solvent at each of the five temperatures, which were accurate at the samples to ∀1 EC. SANS was measured using neutrons with wavelength λ= 5.5 Å, and $\Delta\lambda/\lambda$= 0.11.

Scattered neutrons were detected with a 64 cm H 64 cm two-dimensional position sensitive detector with (128 H 128) pixels and 0.5 cm resolution per pixel. Data reduction was accomplished using Igor Pro software (WaveMetrics, Lake Oswego, OR) with SANS macros developed at the NCNR.[5] Raw counts were put on the same relative scale by normalizing to an incident beam monitor count made by a detector in parallel with the data collection. The scattering then was corrected for empty cell counts, and non-uniform detector response. Data were placed on an absolute scale by normalizing the scattering intensity to the measured incident beam flux. Finally, the data were radially averaged to produce the scattering curves of $I(q)$ versus q □ where $q = (4\pi\lambda)\sin\theta$, and 2θ is the scattering angle measured from the axis of the incoming neutron beam. The sample-to-detector position was 1.0 m with a 25 cm beamstop offset, which, with the 5.5 Å wavelength, provides a q range 0.06 $Å^{-1} < q < 0.63$ $Å^{-1}$, equivalent to a length range of ~100 Å to ~10 Å.

The solution scattering data at each temperature was corrected for its temperature-paired D_2O background by subtracting the solvent scattering scaled by its volume fraction. This method is valid since the sample solution densities in light water could be matched by summing the volumes of water and anhydrous SrI_2 (density 4.55 g cm^{-3}), and this characteristic was extended to the solvent D_2O (1.103 g cm^{-3} at 25 EC)[6]. The fraction subtracted for the 0.5 M solution at each temperature was 0.960 of the pure D_2O scatter.

II.3. *Scattering curve fitting:* The peaks were fit with a Lorentzian function that also accounts for the beamline instrument□s neutron optics□so called smearing of the function. For the Lorentzian equation, the signal magnitude as a function of q in the vicinity of the peak at q_{peak} is

$$I(q) = \frac{A}{1+[(q-q_{peak})/B]^2} + C \qquad (1a)$$

where A is a scaler, q_{peak} the position of the peak, B the half-width at half height, and C the incoherent background. In the fitting, the uncertainties of the three variables are codependent, and these uncertainties vary depending on which of the fitting variables are allowed to change when calculating their best-fitting numerical values.

The Fourier pair of this Lorentzian is the exponential describing decay of the structural correlation, exp(-B≅Δr). Call the correlation length ξ, which substitutes for Δr when 1/e = exp(-B≅ξ). Alternatively, then, Eq. 1a can be rewritten as

$$I(q) = \frac{A}{1+[(q-q_{peak})\xi]^2} + C \qquad (1b)$$

II.4. *Calculating water□s vibrational amplitudes*

For vibrations of H_2O, the classical turning points were estimated in the harmonic approximation with the geometry and force constants determined at the frozen-core CCSD(T)/aug-cc-pVTZ level of theory (coupled-cluster theory with single and double excitations and a perturbative estimate for triple excitations).[7, 8] The numerical results are shown here in Table S1 in the Supplement.

The magnitudes of the ranges shown in the Supplement tables are the differences in relative positions in Ångstroms between the inner and outer turning points. The vibrational frequencies are taken from Shimanouchi.[9] Given the magnitudes of the vibrational frequencies, fewer than 0.3% of the molecules are expected to be in the first excited state.

II.5. *Solution simulations for long-distance structure*

Molecular dynamics simulations have been made to examine the spatial extent of correlations of Sr^{2+} and I^- ions in a 1.18 mol/L aqueous solution at ambient conditions of temperature and pressure. The reported state was chosen to reduce the noise inherent in such results for the relatively small number of ions involved. A different temperature was examined but did not add to understanding.

The simulations were performed in the NPT ensemble [10, 11] for 3760 water molecules, 80 Sr^{2+} ions, and 160 I^- ions. The equations of motion were integrated using a Velocity-Verlet algorithm modified so that the orientational degrees of freedom are described by quaternions. [12, 13] In the NPT formalism, temperature is controlled by separate thermostats for the translational and rotational degrees of freedom. The coupling time for the thermostats is 0.1 ps. The pressure is maintained by a barostat with a coupling time of 1.1 ps. This results in the dimensions of the cubic simulation cell of about 50 Å on a side.

The molecules and ions interact via Coulomb and Lennard-Jones interactions. The Lennard-Jones parameters for the ions were obtained using the Kirkwood-Buff approach as discussed extensively for Sr^{2+} in Naleem et al.[14] and for I^- in Gee et al.[15] The published results for the SPC/E model potential parameters [16] were used for water. The equations of motion are integrated with a time step of 1 fs. In order to obtain equilibrium results a series of eight simulations of 300 ps duration each were run before the ion-ion pair functions for successive runs matched. This was taken to be an indication of equilibration that was required with the long distance of the ion-ion spatial correlations. Then a 500 ps duration run was used to obtain the results reported here.

III. Results and Discussion

III.1. Scattering Curves and Fitting Parameters

A single coherent scattering peak has been observed for SrI_2 in D_2O at ambient temperature, where the concentration dependent q-value at the peak, q_{peak}, indicates average distances between scatterers. These distances were found to range from 11.6 Å for 1 M to 18.4 Å for 0.1 M solutions.[17] Peaks such as these are also called prepeaks,[18, 19] which occur at q values smaller than those associated with local structures within distances less than, say, 4 Å (q = 1.57 Å^{-1}). In order for this scattering to occur, the solution must have a set of distinct scatterers that are correlated in their three-dimensional positions relative to one another. Such structures in solutions have been given a variety of different names: pseudolattice[20], paracrystal[21-23], superarrangement[18], medium-range order, and intermediate-range order.[19] Here, we see scattering from a transient (order of ps) lattice of Sr^{2+} and I^- neighbors the ensemble average of which results in the observed scattering peak at each temperature.

For the SrI_2 solution here, a reasonable expectation was that the structure would be temperature dependent with a decrease in the order as the temperature increases. However, the results here show that the structure remains essentially the same over the full 10 EC to 90 EC range. Figure 1 shows the background-subtracted scattering curves (offset for visibility) for the 0.5 M SrI_2 solution at the temperatures listed. The scattering curves are well fit with Lorentzian curves centered at each peak. The parameters for the Lorentzians are listed in Table I. As can be seen from the values in the fifth column, the best-fit Lorentzian peak widths reported as half widths at half height are sensitive to the values of the other parameters, especially the best-fit baseline. To illustrate this, two different uncertainties are listed there with the smaller one the result when holding A and C of Eq. 1a constant at their optimum values, and the larger uncertainty is found when all the variables are unconstrained.

As noted earlier, the average scatterer separations d is related to the peak by $d = 2\pi/q_{peak}$. The effective molar concentrations can be calculated assuming an array of equally spaced scatterers.[3] To have a distance in Å requires a concentration in Å^{-3}, but it is more convenient to scale to molar measures giving

$$d(\text{Å}) = \frac{12.70}{\sqrt[3]{M}} \qquad (2)$$

where M is the molar concentration. These concentrations are listed in the third column. If the salt were completely dissociated into the Sr^{2+} and I^- ions and equally spaced, the result would show a constant concentration of 1.5 M. Apparently some amount of ion association occurs, although the species present (one or more) cannot be ascertained.

The values of q_{peak} are equal within their uncertainties, but their values do appear to decrease slightly with temperature from 30E to 90E. The calculated average distances and concentrations shown in columns 3 and 4 change accordingly, which points to a possible slight increase in ion association with increasing temperature. Such behavior indicates a small, positive enthalpy of association.

The Fourier transform of the Lorentzian curve is the exponential equation that defines the structural correlation length ξ of the system of scatterers, i.e., 1 = exp(-*B*≅ξ). *B* is the halfwidth at half height of the Lorentzian. The correlation lengths calculated from the best-fit Lorentzians are listed in the rightmost column of Table I. Let us arbitrarily take two times the correlation length as a definition of the positional excursions. At this length, the probability curve has an amplitude that is 13% of the maximum. The two-sided excursion of 2ξ extends about 7 Å (i.e., ∀3.5 Å from the center), approximately the diameter of an ion and its first hydration shell. This narrow range of allowable motion apparently does not change in any systematic way with temperature.

{Figure 1 near here.}

Table I. Lorentzian peak fitting parameters for 0.5 M SrI_2 in D_2O[a]

Temp./EC	q_{peak}/Å^{-1}	*d*, av. scatterer separation[b]/Å	Effective conc.[c]/M	Lorentzian peak half-width[d] /Å^{-1}	Correlation length[e]/Å
10	0.53 ∀ 0.01	11.8 ∀ 0.2	1.25 ∀ 0.07	0.67 ∀ 0.02 (0.2)	1.5
30	0.54 ∀ 0.02	11.6 ∀ 0.4	1.3 ∀ 0.1	0.70 ∀ 0.01 (0.3)	1.4
50	0.51 ∀ 0.02	12.3 ∀ 0.5	1.1 ∀ 0.1	0.54 ∀ 0.02 (0.2)	1.8
70	0.51 ∀ 0.02	12.3 ∀ 0.5	1.1 ∀ 0.1	0.68 ∀ 0.03 (0.4)	1.5
90	0.50 ∀ 0.02	12.6 ∀ 0.5	1.0 ∀ 0.1	0.61 ∀ 0.03 (0.3)	1.6

a. Uncertainties are standard deviations of the parameters for best-fit Lorentzian curves.

b. The relationship between the peak position in *q* in Å^{-1}, and the scatterer separations *d* in Å is $d = 2\pi/q = 6.28/q$.

c. Found from the equation for the distance in Å between equally spaced scatterers in a volume with molar concentration, *M*:[17] $d(Å) = 12.70/M^{1/3}$

d. Uncertainties obtained with background and peak-position best-fit values held fixed. Values in parentheses are uncertainties when the other parameters are unconstrained.

e. An arbitrary but consistent classification of the excursion distance is ∀two times the correlation length, a diameter of four times this correlation length.

III.2. MD Simulations of the ionic solution with long-distance structure

The simulations were intended to investigate whether the long distance correlations (15 Å to 20 Å) could be reproduced. As seen in Figure 2, the spatial extent of the simulated 1.18 M ion-ion pair correlation functions at 25 C extends to 15 Å. This classical MD calculation using these model potentials shows an interion structure at length scales greater than 10 Å that qualitatively matches the properties measured by SANS even though the simulation was done without including proton exchange. The other pair functions involving water-water and water-ions have spatial correlations that extend to less that 10 Å.

We note that the distances investigated here are longer than normally considered in modeling solution structures. However, modeling in such a large space offers the opportunity to find whether the non-hydrolyzing property of SrI_2 is important, and to investigate what chemical properties are necessary to produce such long range structures as well as their persistence in time.

{Figure 2 near here.}

III.3. Reconciling localized ions, conduction, and diffusion

III.3.1 Rotation for transport

The localization of the ions as measured by SANS throughout the temperature range presents a conflict. How can the ionic structure be spatially localized such that the solute ions can scatter neutrons and yet the transport processes of diffusion and ionic conduction still can occur. As was suggested in the initial SrI_2 scattering paper,[17] the apparently stationary structure allowing long-distance motions appears to be consistent only when the ion transport is a consequence of sequential rotations of ion-water constructs with approximately circular cross sections and consisting of the ion bound to *part* of the first hydration layer. The rotation of this partially hydrated ion results in the ion transport and simultaneous solvent countertransport over about 2.5Å. In support of this suggestion, simulations of hydrated ions *in vacuo* indicate that the longest lived, lowest energy structures have anisotropic structures, often with the ion on the outside surface.[24-27] The experimentally determined 7 Å localization requires that the rotating partial shell includes only waters from the first hydration layer,[28] since any significant involvement of a partial second shell would extend the local distance accessible beyond the lengths measured.

This rotational mechanism of transport also clarifies the lack of change with temperature in the structure since there is no need to alter the solution structures significantly over the temperature range. In support of this assertion, the coefficient of thermal expansion of pure (light and heavy) water is temperature dependent, and varies from about $1H10^{-4}$ K^{-1} at 10EC to about $7H10^{-4}$ K^{-1} at 90 EC,[29] and it depends mostly on temperature and only slightly on salt concentration.[30] As a result, the measured ionic structure stays nearly the same over the 80 E range probed here since the solution volume is expected to change less than 4%; the volume in which the molecules and ions can move simply does not change much. Another, interesting

argument against the idea of free volume in water is made by Singh and Dass,[31] where they find that presence of so-called free volume is not consistent with the temperature dependence of numerous physical properties of water.

{Figure 3 near here.}

As interpreted by Ohmine,[32] in liquid water a □free volume□ is a place where the hydrogen bond network is fragile and facile to make a rearrangement and is not a real cavity. Also, as Putintsev has shown[29] the thermal expansion that is seen results mostly from the increased extension of the molecules□ vibrational excursions□ contribution to the anomalous component of the thermal expansion coefficient. That is,

$$c_v - c_{vibr} = T\alpha_2^2 V\gamma_T^{-1} \quad (3)$$

where c_v and c_{vibr} are the heat capacity at constant volume and the vibrational specific heat of water, T is the Kelvin temperature, V the molar volume, and γ_T the isothermal compressibility. The thermal expansion coefficient α is divided into two parts: $\alpha = \alpha_1 + \alpha_2$, the second term of which appears in Eq. 3. The value of α_1 is fixed, and α_2 is temperature dependent and called the anomalous component of the thermal expansion coefficient. (The origin of Equation 1 and details of the entire calculation can be found in the paper cited.) In Figure 3, the results of Putintsev□s calculated values of the anomalous thermal expansion coefficient for both H_2O and D_2O are compared to the values measured by Steckel and Szapiro.[33] Both are in surprising agreement over the 10 EC to 90 EC range used here. The expansion appears due to an apparent increase in molecular size from increased vibrational extension alone. This calculation supports the restraints on ion motion staying constant over the full temperature range.

One caution here is that according to Walrafen,[34] significant changes with temperature in configuration, such as in the numbers of hydrogen bonds between the waters, contributes to changes in c_p.[35, 36] Whether this temperature dependence of the hydrogen bonding network contributes to the anomalous component is unclear, but Eq. 3 is derived from the standard expression $c_p - c_v = T\alpha^2 V\gamma_T^{-1}$. Not having accounted for changes in the hydrogen-bond network may contribute to the poorer fits in Figure 3 at the higher temperatures.

Nevertheless, the rotation mechanism for transport conforms to the important and widely recognized fact that rotation and translation are tightly coupled in water.[37-40] Proof for this understanding can be found from experiments that are described in the next section.

III.3.2. Picosecond H-bond exchange

One further problem in analyzing transport in water is that the protons are exchanging between the two minima of a double-well potential between oxygens about every 1 ps. From experiments, the distance between the minima is 0.63 Å,[41] and that varies by the strength of the H-bond.[42, 43] The ps timescale for exchange as has been determined most directly by THz spectrometry of isolated water clusters.[44] Because of the fast exchange, within liquid water these proton ps exchanges create an incredibly complicated dance[32, 39, 40, 45-48] and, as a result, thinking

of the unit H_2O as an individual, always-intact molecule seems difficult to support both for simulations and interpretations of experimental data. (In the discussion of these fast events, experimental work on HOD in either H_2O or D_2O will not be included, since the vibrational mode coupling as well as proton or deuteron exchange differ from the isotopically pure liquids.[49])

The consequences of this more appropriate view of liquid water as consisting of proton exchanges only indirectly connected with Ångstrom-length oxygen transport are broad. For example, it suggests a reinterpretation of some reported quasielastic neutron scattering (QENS) experiments. The earliest were those of Irish,[50] where the magnitude of the measured motion was interpreted as a hydrogen RMS displacement distance of 0.6 Å. This was the same in water and ice. This distance equals the distance between the double-well minima noted above. Additional analysis was done on the data to find a self diffusion coefficient for the liquid, but this required the faulty assumption that rotation and translation are not coupled. However, as noted earlier, at times longer than 1 ps, the rotations and translations are strongly coupled.[37, 39, 40, 51] This latter point is also seen in MD simulations. [51] Other QENS papers also assumed translation decoupled from rotation,[52-54] and so their derived parameters for both translation and rotation are expected to be inapplicable as well.

The picosecond H-bond exchange also should cause reinterpretation where Teixeira et al.[53] notes that the motions of the protons can be well approximated as a Debye-Waller factor assigned to apply for the protons mean-square vibrational amplitude transverse to the hydrogen bonds. The associated extent was 0.484 Å. However, even for isolated waters, without the restraint of H-bonding, results from the calculations shown in Supplement 1 indicate that the two classical turning points for the bending mode are 0.2 Å apart, the value of which is an *upper* limit for a RMS displacement. The calculated ~0.484 Å displacement is closer to the 0.6 Å spacing of the double-well minima than to a vibrational displacement.

III.4. Rotation or Pseudorotation?

The idea that transport together with simultaneous solvent countertransport by rotation both minimizes the disruption of the surrounding framework while simultaneously having a strong coupling between rotation and translation suggests that rotation should be considered as a general mechanism for transport in condensed media. Below, we present arguments for that viewpoint derived from published experimental results.

III.4.1 Requirements for rotation of molecular waters

{Figure 4 near here.}

In the remarks made above, descriptions of various rotations have been vague. One important reason is that interpretations of experiments of water and its solutions with molecular rotations are greatly confounded by pseudorotations as described in greater detail below.

But first, let us consider what is involved to have an intact water molecule actually rotate. The rotation of a durable, always-intact water molecule in the liquid has been treated theoretically, and only one team's detailed work has been chosen for comparison.[55, 56] For an intact molecule to rotate freely, there can be at most only one hydrogen bond intact, as shown in Figure 4. The molecule can only spin around the remaining hydrogen bond, and a number of H-bonds must be broken for that rotatable structure to appear.

The number of bonds broken need not be three. Numerous simulations indicate the initial number of bonds is not exactly four and is temperature dependent,[55, 56] which is mostly in agreement with some experiments.[34, 57, 58] This is confounded by Robinson et al.[59] asserting two different picosecond-rearranging local icelike structures. The activation energy can be decreased somewhat to the extent that the rotating molecule can slide between adjacent neighbor oxygens that, in essence, a make-before-break mechanism as found from simulations by Laage and Hynes.[55] In any case, this rotational process can be classified as a *single-proton exchange*.

An interesting question to ask is, How fast would a water molecule rotate if it were not encased in a hydrogen bonding network? This question was answered experimentally by Graener et al.[60] with picosecond time- and polarization-resolved infrared double resonance spectrometry of monomeric water in organic solvents that have varying hydrogen bonding abilities. The water reorientational relaxation time τ_R (for exponential decay) increases from poorly hydrogen bonding $CHCl_3$ of 1.7 ps to moderately hydrogen bonding CH_3CN of 6.0 ps. From the shifts in the OH frequencies, the binding energies for the hydrogen bonds are estimated to vary from a low of 1.2 kcal mol^{-1} to a high for CH_3CN of 2.0 kcal mol^{-1}. (1 kcal = 4.184 kJ.)

Rotational correlation times have been interpreted for a number of types of experiments as if intact waters were rotating in this way. However, another mechanism can confound this conventional interpretation in liquid water: pseudorotation, the mechanism of which is illustrated in Figure 5 and is the subject of the following section.

III.4.2. Pseudorotations

In liquid water, a pseudorotation arises from dual proton exchanges of hydrogen-bonded protons to and from an oxygen. This is illustrated in Figure 5, where both protons of the exchange move radially relative to the oxygen. Pseudorotation may be defined as a low-energy, alternative pathway to *apparent* fast molecular rotation. (Apart from liquid water, a number of different molecular mechanisms can cause pseudorotations both with and absent bond breaking.[61, 62])

{Figure 5 near here.}

The water pseudorotation is over an angle of 105E. (If a rotational correlation time is taken for a rotation of one radian, the pseudorotation is nearly twice that angle.) In addition to the pseudorotation from the dual proton exchange, the water exhibits a small pseudotranslation. The center of mass of the H_2O moiety lies on the bisector of the protons at 0.065 Å from the oxygen nucleus. As a result, when the dual proton exchange occurs, the center of mass moves linearly 0.10 Å while switching the bisector angle by 105E. This small pseudotranslation is the apparent center of mass movement that can occur with a stationary oxygen.

Both of the approximately simultaneous radial exchanges occur on the picosecond time scale. Because of the tetrahedral symmetry, every dual exchange is equivalent. If we assume that the dual exchange must be exactly coincidental, an approximation would be that there are four hydrogen bonds exchanging every picosecond of which two of them must exchange at the same time. In other words this dual exchange will occur in a period ${}_4C_2 = 4!/2!2! = 6$ ps. This will set the upper limit of time, since if a dual exchange appears as a pseudorotation for a wider range of times, the increased probability of its occurrence decreases the apparent rotational time toward the single picosecond range.

Following are two examples where measured apparent rotation times are much faster than the rotation times of the solitary waters in organic solvents noted above. Explaining these measurements as being of pseudorotations is reasonable. In the first, the temperature of Rayleigh depolarization was used to probe the rotation of a dipole vector in liquid water.[63] The □B□ process had relaxation times τ_B and activation energy 2.7 kcal mol^{-1}. Both the E_a and relaxation times were attributed to H-bond lifetimes and activation, and the authors suggested their measurements □justifies why translational diffusion and molecular rotations are strongly related.□ Here, we suggest that they were observing pseudorotations.

In the second, Bakker and Skinner[64] measured subpicosecond changes in the OH stretching region with femtosecond mid-IR pump and probe pulses. The partial decay of the anisotropy due to librations is nearly complete after 100 fs. They find an absorption anisotropy decay time of 2.5∀0.2 ps, for which a relatively involved explanation was made involving, *inter alia*, rearrangement of the water network. A more straightforward interpretation can be they are observing the normal properties of pseudorotations.

The occurrence of pseudorotation has underlying it two physical properties: the protons in water are exchanging on the picosecond timescale, and the low-energy paths for reactions are those that require minimum changes to the remainder of the water environment. It is interesting to consider briefly that these two characteristics should apply to water diffusion itself, which is the subject of the next section.

III.4.3. Does a Rotational Mechanism Apply to Pure Water Transport?

As noted in Section III.3.2, translation and rotation are coupled in water together with the picosecond hydrogen exchange. In addition, pseudorotation will not couple with oxygen migration, so an alternative mechanism must be present. Can the idea of rotation of a molecular grouping with a circular cross section apply to water transport itself?

Rotation with minimum disturbance of the surrounding molecules suggests the presence of transient water multimers with circular shapes rotating about their highest symmetry axis, which subsequently suggests planar water polygons: trimers, pentamers, and hexamers.[27] As a representative example, let us consider only trimers, which are well established to be relatively stable.[62, 65-69] The trimer has three internal, equatorial hydrogen bonds and only three hydrogens projecting out of the plane of the ring, two in one direction and one opposite. The internal hydrogen bonds between the oxygens in the gas-phase trimer exchange in less than 2 ps,[44] and the trimer is known to rotate freely in *solid* noble gas matrices.[62] In liquid water, the transient trimer would be free to rotate by releasing the three external hydrogen bonds, and the next triple H-bond position would be equivalent after traveling the trimer□s oxygen-oxygen distance of about 2.85 Å without needing any perturbation of the waters beyond the H-bonds to the nearest neighbors. Finally, a rotating trimer then can break up and allow the oxygen members to join new trimers that rotate, and so forth. This process would have the appearance of continuous transport at times greater than about 10 ps.[32] In other words, the trimer could be free to rotate multi-Ångstrom distances around its axis by breaking the same number of H-bonds as required for the water monomer alone illustrated in Figure 4.

III.4.4. Does the Picosecond Proton Exchange in Water Control the NMR Relaxation Time in Solutions of Paramagnetic Ions?

Nearly sixty years ago, Bloembergen and Morgan[70] considered the possible dominant mechanism for proton relaxation times in aqueous solutions of Mn^{2+} and V^{2+}. They considered the correlation times for dipolar exchange and spin exchange, the rate of chemical exchange of protons from the ion hydration shell, the electron spin relaxation, and the rate of tumbling. They conclude that the proton relaxation time depends on the relaxation time of the electron spins, and that relaxation time was dependent on the distortion of the hydrated metal complex by the surrounding waters. In a Mn^{2+} solution, they estimated the characteristic time for that perturbation to be 2.8 ps at 21 °C and for V^{2+} at the same temperature the perturbation rate was 1.60 ps with an E_a of 3.9 kcal mol^{-1}. (Earlier, Al'tshuler [71] suggested that the perturbations occurred from vibrational modes in the system.) We note that the activation energy for proton conductivity[Robinson, 1959; Cornish, 1984] is in the range 2.4 to 2.8 kcal mol^{-1} while E_a for self-diffusion of water[72] is 4.3 kcal mol^{-1}. Both the characteristic times and activation energies lead us to suggest that the ps proton exchange/pseudorotation is involved as the distortion.

III.4.5. Difficulties with Rotation and H-Exchange Determined by NMR with ^{17}O

It seems reasonable that a more detailed understanding of the water-ion transport through a rotational mechanism could be obtained from NMR measurements involving ^{17}O such as have

been carried out since the early days of NMR development.[73] From measuring relaxation rates in the presence of water enriched in ^{17}O, in his pioneering work, Meiboom found for acidic and basic conditions, respectively,[73]

$H_2O + \mathbf{H}H_2O^+ \; 6 \; \mathbf{H}H_2O^+ + H_2O$; $k_1 = (10.6 \forall 4)\ H\ 10^9\ L\ mol^{-1}\ s^{-1}$

$\mathbf{H}^*OH + OH^- \; 6 \; OH^{--} + \mathbf{H}OH$; $k_2 = (3.8 \forall 1._5)\ H\ 10^9\ L\ mol^{-1}\ s^{-1}$

where the rate constants are corrected for quadrupole relaxation. The equation derived to quantify the exchange rate of a hydrogen atom, τ^{-1}, is

$$\tau^{-1} = \tfrac{1}{3} k_1[H^+] + \tfrac{1}{2} k_2 \left(K_W / [H^+] \right) \qquad (4)$$

where the fractions are statistical factors. The dissociation constant of water at 25 EC, $K_W = 10^{-14}$ $mol^2\ L^{-2}$, and at pH 7, $[H^+] = 10^{-7}$. With these substitutions and the listed rate constants, we find $\tau^{-1} = 5._4\ H\ 10^2\ s^{-1}$, or, alternatively, an exchange lifetime $\tau = 2$ ms at 25$\forall$1 EC and pH 7.

An additional chemical argument can be made for the improbable exchange times found from the ^{17}O-substituted NMR measurements. We take the example of ^{17}O-water attached to paramagnetic Gd^{3+} complexes of the type used for relaxation agents in MRI. The data fitting equations yield the complexes rotational correlation times τ_R as well as the average residence times τ_M for one or two water ligands assumed to be molecular $^{17}OH_n$ bound on the metal ion. Table II shows a few examples of the parameter values found by Rojas-Quijano, et al.[74]

Table II. Paramagnetic contrast agents properties by NMR from reference [74]

	Residence time $^{17}OH_n$	Rot. correlation time	Ratio τ_M/τ_R
Complex 3	0.71 $\forall$ 0.09 μs	141 $\forall$ 3 ps	$5._0\ H\ 10^3$
Complex 6	0.66 $\forall$ 0.05 μs	86 $\forall$ 2 ps	$7._7\ H\ 10^3$
Complex 8	1.3 μs	70 ps	$18\ H\ 10^3$

Since the chemistry of rotation in water involves breaking and making hydrogen bonds, let us make a reasonable assumption that for the rotation of the hydrated paramagnetic ion the bound water also forms and breaks hydrogen bonds but *only one time* over each rotational correlation time. Then it must follow that a proton on the bound water does not exchange with an adjacent water even once in over 5,000 hydrogen bond formations/breaks.

The chemistries of the fast hydrogen exchange between oxygens in water even if slowed down by two orders of magnitude are not reconcilable with these calculated water residence times. A wished-for unified viewpoint also must include the additional factor that the protons of the bound water will be made more acidic by the trivalent-ion binding.[75] From the numbers discussed in this section, it appears that NMR results as currently interpreted are discordant and cannot contribute to understanding more details of the rotation of anisotropic ion-water clusters in solution.

IV. Summary and Conclusions

Coherent small angle neutron scattering obtained from a 0.5 M solution of the non-hydrolyzing salt SrI_2 at five temperatures from 10 °C to 90 °C surprisingly shows almost no change in solution structure over that temperature range. The real-space positions between the scatterers are shown to be constrained in a remarkably narrow region about 7 Å across. The long-distance order of this ionic solution was able to be simulated with molecular dynamics calculations, and was found to rely on the entire population of the hydrated species.

A fascinating question arises as to how diffusion and conduction can occur with such localization, and the suggested answer is that rotation of water-ion assymetric clusters can explain such motion with counter flow while minimally disturbing the remainder of the surroundings. The idea of free volume models for diffusion are countered by the ability of vibrational extensions to explain the temperature dependent expansion of water.

Because proton exchange occurs on the picosecond timescale, water should not be considered to be an always-intact molecule. With such fast exchange, a dual exchange can also occur in the picosecond time range and will produce a pseudorotation□the appearance of a rotation□of, e.g., the dipole vector. The hopping of the hydrogens between the two wells of the hydrogen bond potential together with pseudorotation appear to offer alternative explanations of the molecular origins of numerous types of experiments.

Acknowledgements

Access to SANS instruments was provided by the Center for High Resolution Neutron Scattering, a partnership between the National Institute of Standards and Technology and the National Science Foundation under Agreement No. DMR-1508249. Raw data were generated at the NIST Center for Neutron Research. Derived data supporting the findings of this study are available from the corresponding author upon reasonable request. Data can be accessed at ftp://129.6.120.51/pub/sansdata. Thanks to Karl Irikura with the aid of Prof. J. F. Stanton for the vibration displacement calculations, and Dennis Torchia , Craig Brown, Susan Krueger, Alex Grishaev, Curt Meuse, Robert Brinson, Joseph Curtis, Paul Butler, Steve Kline, and Tom Allison for helpful discussions.

Disclaimer

*Certain trade names and company products are identified in order to specify adequately the procedure. In no case does such identification imply recommendation or endorsement by the National Institute of Standards and Technology, nor does it imply that the products are necessarily the best for the purpose.

References

1. K. A. Rubinson, *Protein J.*, 2019, **38**, 95-119.
2. F. Zernike and J. A. Prins, *Z. Phys.*, 1927, **41**, 184-194.
3. K. A. Rubinson, *Anal. Methods*, 2017, **9**, 2744-2750.
4. C. J. Glinka, J. G. Barker, B. Hammouda, S. Krueger, J. J. Moyer and W. J. Orts, *J. Appl. Cryst.*, 1998, **31**, 430-445.
5. S. R. Kline, *J. Appl. Cryst.*, 2006, **39**, 895-900.
6. F. J. Millero, R. Dexter and E. Hoff, *J. Chem. & Engin. Data*, 1971, **16**, 85-87.
7. R. A. Kendall and T. H. Dunning Jr., *J. Chem. Phys.*, 1992, **96**, 6796-6806.
8. K. Raghavachari, G. W. Trucks, J. A. Pople and M. Head-Gordon, *Chem. Phys. Lett.*, 1989, **157**, 479-483.
9. T. Shimanouchi, *Tables of Molecular Vibrational Frequencies Consolidated, Volume I*, National Bureau of Standards, 1972.
10. M. E. Tuckerman, Y. Liu, G. Ciccotti and G. J. Martyna, *J. Chem. Phys.*, 2001, **115**, 1678-1702.
11. G. J. Martyna, D. J. Tobias and M. L. Klein, *J. Chem. Phys.*, 1994, **101**, 4177-4189.
12. D. J. Evans and S. Murad, *Mol. Phys.*, 1977, **34**, 327-331.
13. N. Martys and R. D. Mountain, *Phys. Rev. E*, 1999, **59**, 3733-3786.
14. N. Naleem, N. Bentenitis and P. E. Smith, *J. Chem. Phys.*, 2018, **148**, 222828.
15. M. B. Gee, N. R. Cox, Y. Jiao, N. Bentenitis, S. Weerasinghe and P. E. Smith, *J. Chem. Theory. Comput.*, 2010, **7**, 1369-1380.
16. H. J. C. Berendsen, J. R. Grigera and T. P. Straatsma, *J. Phys. Chem.*, 1987, **91**, 6269-6271.
17. K. A. Rubinson, *J. Soln. Chem.*, 2014, **43**, 453-464.
18. J. A. Prins, *J. Chem. Phys.*, 1935, **3**, 72-80.
19. M. A. Marques, M. I. d. B. Marques, M. I. Cabaço, A. M. Gaspar, M. P. M. Marques, A. M. Amado and A. M. A. da Costa, *J. Mol. Liqs.*, 2007, **134**, 142-150.
20. L. M. Varela, J. Carrete, M. García, L. J. Gallego, M. Turmine, E. Rilo and O. Cabeza, *Fluid Phase Equilib.*, 2010, **298**, 280-286.
21. R. Brämer and W. Ruland, *Makromol. Chem.*, 1976, **177**, 3601-3617.
22. H. Matsuoka, H. Tanaka, T. Hashimoto and N. Ise, *Phys. Rev. B*, 1987, **36**, 1754-1765.
23. H. Matsuoka, H. Tanaka, N. Iizuke, T. Hashimoto and N. Ise, *Phys Rev. B.*, 1990, **41**, 3854-3856.
24. B. Hartke, A. Charvat, M. Riech and B. Abel, *J. Chem. Phys.*, 2002, **116**, 3588-3600.
25. A. Khan, *Chem. Phys. Lett.*, 2004, **388**, 342-347.
26. F. Schulz and B. Hartke, *Theor. Chem. Acc*, 2005, **114**, 357-379.
27. A. S. Zatula, M. J. Ryding, P. U. Andersson and E. Uggerud, *Int. J. Mass Spec.*, 2012, **330-332**, 191-199.
28. H. G. Hertz and R. Mills, *J. Chem. Phys. (Paris)*, 1976, **73**, 499-508.
29. N. M. Putintsev, *Russian J. Phys. Chem.*, 1982, **56**, 1403-1404.
30. H. U. Sverdrup, M. W. Johnson and R. H. Fleming, *The Oceans Their Physics, Chemistry, and General Biology*, Prentice-Hall, New York, 1942.
31. O. Singh and N. Dass, *Indian J. Pure & Appl. Phys.*, 1971, **9**, 92-94.
32. I. Ohmine, *J. Phys. Chem.*, 1995, **99**, 6767-6776.
33. F. Steckel and S. Szapiro, *Trans. Farad. Soc.*, 1963, **59**, 331-343.
34. G. E. Walrafen, in *Water: A Comprehensive Treatise*, ed. F. Franks, 1972, vol. 1 ch. 5,

pp. 151-214.
35. V. S. Langford, A. J. McKinley and T. I. Quickenden, *J. Phys. Chem. A.*, 2001, **105**, 8916-8921.
36. G. P. Johari, *J. Chem. Phys.*, 2007, **126**, 114901.
37. M. Holz, X.-a. Mao, D. Seiferling and A. Sacco, *J. Chem. Phys.*, 1996, **104**, 669-679.
38. D. Di Cola, A. Deriu, M. Sampoli and A. Torcini, *J. Chem. Phys.*, 1996, **104**, 4223-4232.
39. V. I. Arkhipov and N. Agmon, *Israel J. Chem.*, 2003, **43**, 363-371.
40. N. Agmon, *Acc.. Chem. Res.*, 2011, 63-73.
41. P.-G. Jönsson, *Acta Cryst.*, 1971, **B27**, 893-898.
42. B. Schiøtt, B. B. Iversen, M. G. K. H., F. K. Larsen and C. Bruice, *Proc. Natl. Acad. Sci. USA*, 1998, **95**, 12799012802.
43. G. Gilli and P. Gilli, *J. Mol. Struct.*, 2000, **552**, 1-15.
44. F. N. Keutsch and R. J. Saykally, *Proc. Natl. Acad. Sci. USA*, 2001, **98**, 10533-10540.
45. B. E. Conway, *Annu. Rev. Phys. Chem.*, 1966, **17**, 481-528.
46. R. Laenen, K. Simeonidis and A. Laubereau, *Bull. Chem. Soc. Jpn.*, 2002, **75**, 925-932.
47. P. Wernet, D. Nordlund, U. Bergmann, M. Cavalleri, M. Odelius, H. Ogasawara, L. Å. Näslund, T. K. Hirsch, L. Ojamäe, P. Glatzel, L. G. M. Pettersson and A. Nilsson, *Science*, 2004, **304**, 995-999.
48. S. Garrett-Roe, F. Perakis, F. Rao and P. Hamm, *J. Phys. Chem. B*, 2011, **115**, 6976-6984.
49. H. Weingärtner, *Zeit. Physik. Chem. NF*, 1982, **13$_2$O$_2$2**, 129-149.
50. J. D. Irish, W. G. Graham and P. A. Egelstaff, *Can. J. Phys.*, 1978, **56**, 373-380.
51. D. Di Cola, A. Deriu, M. Sampoli and A. Torcini, *J. Chem. Phys.*, 1996, **104**, 4223-4232.
52. K. E. Larsson, *Phys Rev. A*, 1971, **3**, 1006-1022.
53. J. Teixeira, M.-C. Bellissent-Funel, S. H. Chen and A. J. Dianoux, *Phys. Rev.A.*, 1985, **31**, 1013-1917.
54. A. Consolo, A. Orecchini, C. Petrillo and F. Sacchetti, *J. Phys. Chem. B*, 2010, **114**, 16713-16717.
55. D. Laage and J. T. Hynes, *Science*, 2006, **311**, 832-835.
56. D. Laage, g. Stirnemann, F. Sterpone, R. Rey and T. Hynes, *Ann. Rev. Phys. Chem.*, 2011, **62**, 395-416.
57. J. R. Scherer, M. K. Go and S. Kint, *J. Phys. Chem.*, 1974, **78**, 1304-1313.
58. C. Huang, K. T. Wikfeldt, T. Tokushima, D. Nordlund, Y. Harada, U. Bergmann, M. Niebuhr, T. M. Weiss, Y. Horikawa, M. Leetmaa, M. P. Ljungberg, O. Takahashi, A. Lenz, L. Ojamäe, A. P. Lyubartsev, S. Shin, L. G. M. Pettersson and A. Nilsson, *Proc. Natl. Acad. Sci.*, 2009, **106**, 15214-15218.
59. G. W. Robinson, C. H. Cho and J. Urquidi, *J. Chem. Phys.*, 1999, **111**.
60. H. Graener, G. Seifert and A. Laubereau, *Chem. Phys.*, 1993, **175**, 193-204.
61. H. L. Strauss, *Ann. Rev. Phys. Chem.*, 1983, **34**, 301-328.
62. J. Ceponkus, A. Engdahl, P. Uvdal and B. Nelander, 2013.
63. O. Conde and J. Teixeira, *J. Physique*, 1983, **44**, 525-529.
64. H. J. Bakker and J. L. Skinner, *Chem. Rev.*, 2010, **110**, 1498-1517.
65. K. Liu, J. G. Loeser, M. J. Elrod, B. C. Host, J. A. Rzepiela, N. Pugliano and R. J. Saykally, *J. Am. Chem. Soc.*, 1994, **116**, 3507-3512.
66. J. K. Gregory and D. C. Clary, *J. Phys. Chem.*, 1996, **100**, 18014-18022.
67. M. R. Viant, J. D. Cruzan, D. D. Lucas, M. G. Brown, K. Liu and R. J. Saykally, *J. Phys. Chem. A.*, 1997, **101**, 9032-9041.
68. M. Ortiz-Repiso, R. Escribano and P. C. Gómez, *J. Phys. Chem. A*, 2000, **104**, 600-609.
69. S. K. Reddy, S. C. Straight, P. Bajaj, C. H. Pham, M. Riera, D. R. Moberg, M. A. Morales, C. Knight, A. W. Götz and F. Paesani, *J. Chem. Phys.*, 2016, **145**, 194504.

70. N. Bloembergen and L. O. Morgan, *J. Chem. Phys.*, 1961, **34**, 842-850.
71. S. A. Al'tshuler and K. A. Valiev, *Soviet Phys. JETP*, 1959, **35**, 661-668.
72. R. Mills, *J. Phys. Chem.*, 1973, **77**, 685-688.
73. S. Meiboom, *J. Chem. Phys.*, 1961, **34**, 375-388.
74. F. A. Rojas-Quijano, G. Tircsó, E. T. Benyó, Z. Baranyai, H. T. Hoang, F. Kálmán, P. K. Gulaka, V. D. Kodibagkar, S. Aime, Z. Kovács and D. Dean Sherry, *Chem.: Eur. J.*, 2012, **18**, 9669-9676.
75. S. Aime, A. Barge, M. Botta, D. Parker and A. S. De_Sousa, *J. Am. Chem. Soc.*, 1997, **119**, 4767-4768.

Figure captions

Figure 1. SANS data and Lorentzian fits for a 0.5 M SrI_2 solution in D_2O at the five temperatures listed. The model-curve parameters are listed in Table I. The uncertainties shown are for the counting statistics only.

Figure 2. Radial pair-correlation functions for the ions of SrI_2 calculated from MD simulations.

Figure 3. Temperature dependence of the thermal expansion coefficients for H_2O and D_2O measured and calculated including the contributions from active vibrational modes of the waters.

Figure 4. Intact-molecule rotation in liquid water is difficult. The eventual rotation may be viewed as one proton switching oxygen neighbors.

Figure 5. Pseudorotation of the center water molecule by dual proton transfer. The leaving proton binds to an oxygen in front (not pictured) while the arriving proton comes from a different oxygen, the water adjacent to the right.

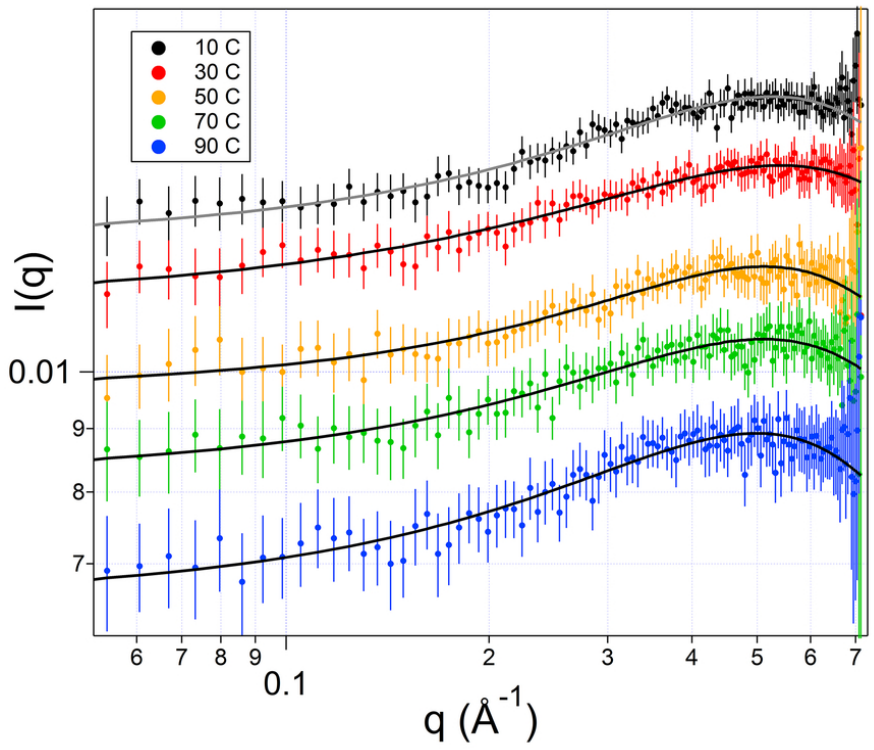

Figure 1. SANS data and Lorentzian fits for a 0.5 M SrI_2 solution in D2O at the five temperatures listed. The model-curve parameters are listed in Table I. The uncertainties shown are for the counting statistics only.

82x65mm (300 x 300 DPI)

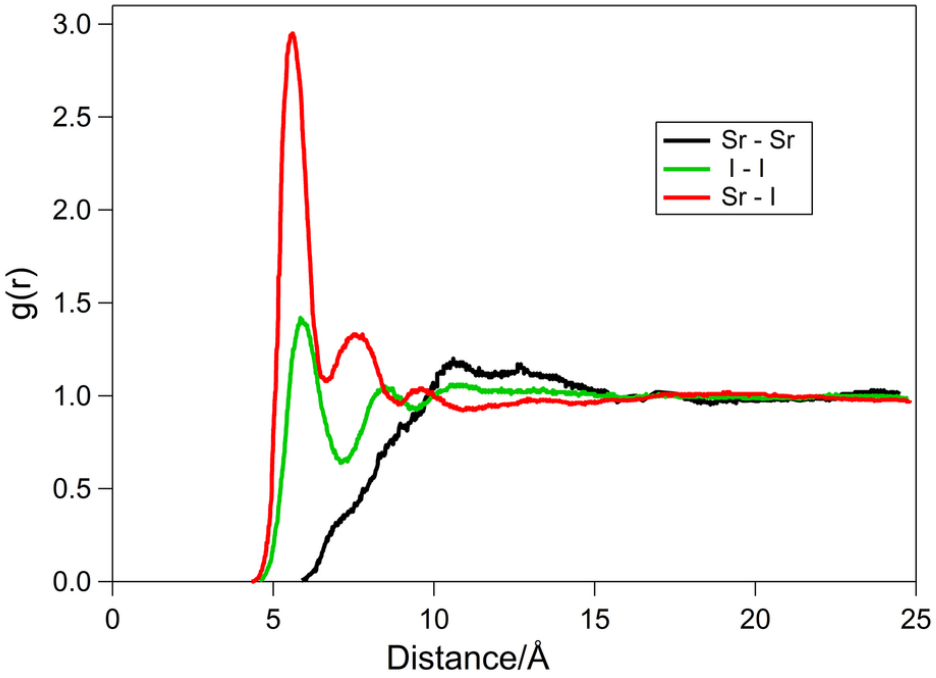

Figure 2. Radial pair-correlation functions for the ions of SrI_2 calculated from MD simulations.

82x58mm (300 x 300 DPI)

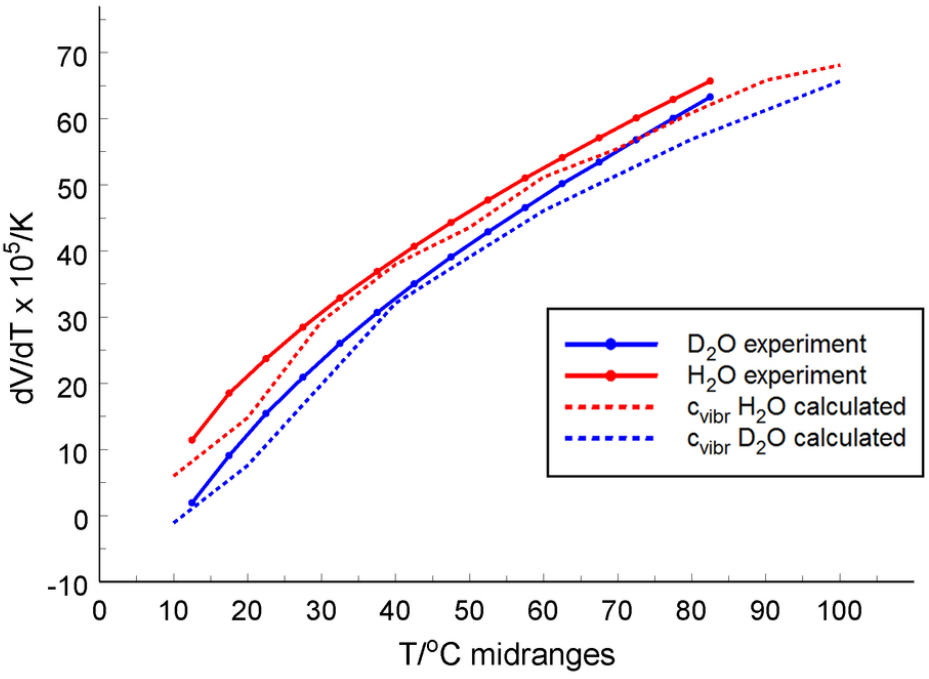

Figure 3. Temperature dependence of the thermal expansion coefficients for H_2O and $D2_O$ measured and calculated including the contributions from active vibrational modes of the waters.

82x58mm (300 x 300 DPI)

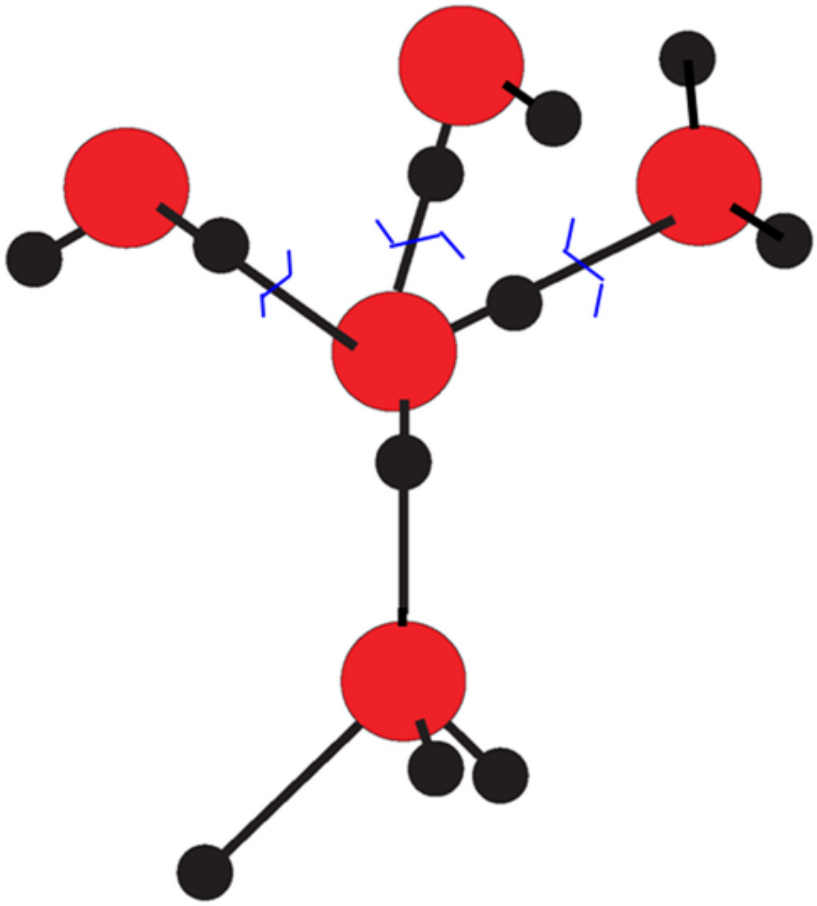

Figure 4. Intact-molecule rotation in liquid water is difficult. The eventual rotation may be viewed as one proton switching oxygen neighbors.

50x52mm (300 x 300 DPI)

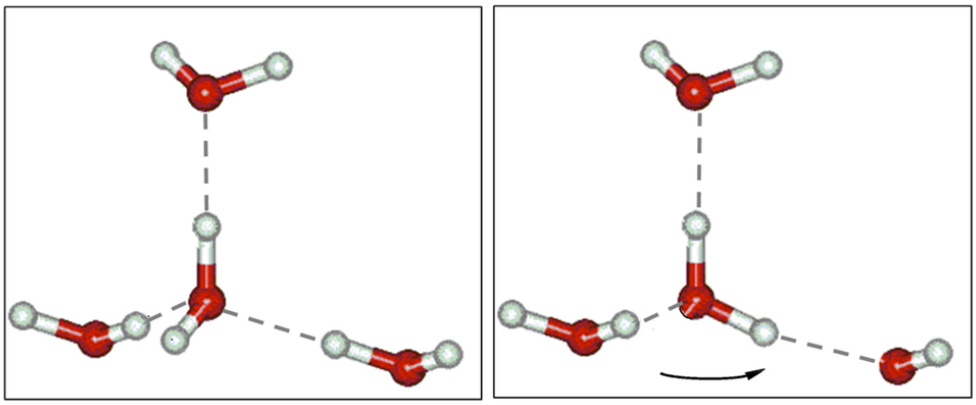

Figure 5. Pseudorotation of the center water molecule by dual proton transfer. The leaving proton binds to an oxygen in front (not pictured) while the arriving proton comes from a different oxygen, the water adjacent to the right.

82x35mm (300 x 300 DPI)

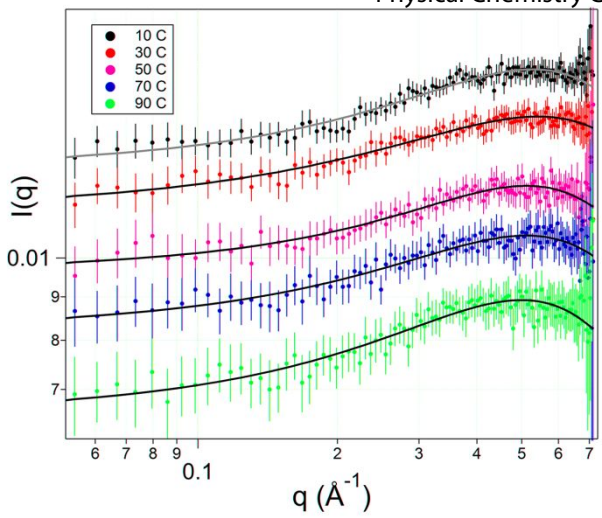

Rubinson

Table of Contents Entry

SrI_2 ions at 0.8 M in water are present with a structure that can scatter neutrons, and, within experimental uncertainty, the structure does not change between 10ā C and 90ā C, showing an organization that must be reconciled with ionic transport.